Data Supplement for:

Connective Tissue Growth Factor Regulates Cardiac Function and Fibrosis in a Transgenic Mouse Model of Dilated Cardiomyopathy

SUPPLEMENTAL METHODS

Materials and reagents. Real-time qPCR reagents were obtained from GE Healthcare Biosciences (Piscataway, NJ), and Invitrogen (Grand Island, NY). cDNA primers used in genotyping were obtained from Integrated DNA Technologies, Inc. (Coralville, IA). PKCε monoclonal antibody (mAb) was obtained from BD Biosciences (Cat #610085; San Jose, CA). GAPDH mAb was from Novus Biologicals (Cat #NB300-221; Littleton, CO). CTGF mAb was obtained from Santa Cruz Biotechnology (Cat #sc-101586; Santa Cruz, CA). Phospho-specific cMyBP-C Ser302 and total cMyBP-C polyclonal antibodies (pAb) were a kind gift from Dr. Sakthivel Sadayappan (Loyola University Chicago, Maywood, IL). Phospho-specific cTnI Thr143 (Cat #ab58546) and total cTnI mAb (Cat #ab47003) were from Abcam Cambridge, MA). Horseradish peroxidase-conjugated goat anti-rabbit (Cat #1706515) and goat anti-mouse (Cat #1721011) IgG were obtained from Bio-Rad (Hercules, CA). All other reagents were of the highest grade commercially available and were obtained from Sigma, and Baxter S/P (McGaw Park, IL).

Echocardiography. Transthoracic M-mode and 2D echocardiography was performed on anesthetized mice using an Acuson 15L8 Microson High-Resolution Transducer and Acuson Sequoia C256 Echocardiography System (Siemens Medical Solutions; Malvern, PA). Anesthesia was induced in a closed container with isoflurane (5% in O_2) and maintained with 2% isoflurane by nosecone delivery. Temperature was maintained by placing animals in the supine position on a 37ºC heated table. Parasternal long- and short-axis images at the level of the papillary muscles were analyzed in real-time or saved on 230Mb magneto-optical discs for off-line analysis. Interventricular septal thickness, LV posterior wall thickness, and LV internal dimension were measured at the end of diastole (d) and systole at maximum sweep speed. LV fractional shortening (FS, %) was calculated from digital images as ((LV end-diastolic dimension – LV end-systolic dimension) / LV end-diastolic dimension) x 10^2. End-systolic, end-diastolic, and stroke volumes (LVESV, LVEDV, and LVSV in µL, respectively) were estimated using the spherical formula. LV ejection fraction (EF, %) was calculated as (LVSV / LVEDV) x 10^2. LV mass (mg) was calculated as LV tissue volume (mm^3) x 1.04. LV Relative Wall Thickness was calculated as 2 x (LV PW thickness,d / LV internal dimension,d). Left atrial area (mm^2) was measured using the tracing function from the parasternal long-axis image. LV Remodeling Index (LVRI, mg/µL) was calculated as the ratio of LV mass to LV volume.

LV catheterization. LV catheterization was performed on anesthetized mice using a 1.4F Millar Pressure-Volume Catheter (SPR-839, Millar Instruments, Houston, TX) connected to an MPVS-300 System and interfaced to a PowerLab 8/35 High-Performance Data Acquisition System (ADInstruments, Colorado Springs, CO). A neck cut-down was performed under general anesthesia and an 18g catheter was inserted into the trachea, which was connected to a Harvard Model 687 mouse ventilator set to deliver ~200µl tidal volume at 145 respirations per min. A midline incision just below the diaphragm was used to expose the LV apex, which was punctured with a 30g needle in order to introduce the conductance catheter under direct visualization. Pressure and volume measurements were acquired and analyzed using PVAN software.

Detailed mRNA expression analysis methods. Total RNA was isolated from frozen LV tissue using TRIzol Reagent (Life Technologies, Carlsbad, CA) and purified on RNeasy Mini Spin Columns (Qiagen, Valencia, CA) with on-column DNase digestion to remove residual genomic DNA. RNA quantity and quality were assessed using an ND-1000 spectrophotometer (NanoDrop Technologies, Wilmington, DE) and 2100 Bioanalyzer (Agilent Technologies, Palo Alto, CA), with all samples having optical density ($OD_{260/280}$) ratios ≥ 1.9 and RNA integrity (RIN) values ≥ 6.7.

For quantitative RT-PCR analyses, cDNA was prepared from 2 µg of total RNA using SuperScript Reverse Transcriptase (Invitrogen) or the High Capacity cDNA Reverse Transcription Kit (Life Technologies). In some quantitative PCR reactions, samples were run in triplicate on an ABI 7300 Real-Time PCR System (Applied Biosystems, Foster City, CA), using TaqMan® assays for Col1a1 (Mm00801666_g1), Col3a1 (Mm01254476_m1), Ctgf (Mm01192933_g1), and eukaryotic 18S ribosomal RNA (4352930E). In other experiments, samples were analyzed in triplicate on a 7900HT Fast Real-Time PCR System using PerfeCTa qPCR FastMix with UNG and ROX (VWR, Visalia, CA) or Platinum Quantitative PCR SuperMix-UDG (Life Technologies) with TaqMan® assays for 18S ribosomal RNA (4319413E), Actb (4352341E), Col1a1 (Mm00801666_g1), Col1a2 (Mm00483888_m1), Col3a1 (Mm01254476_m1), Col5a2 (Mm00483675_m1), Ctgf (Mm00515790_g1), Fbn1 (Mm00514908_m1), Lox (Mm00495386_m1), Ltbp2 (Mm01307379_m1), Mfap5 (Mm00489404_m1), Postn (Mm00450111_m1), Serpine2 (Mm00436753_m1), Tgfb3 (Mm00436960_m1) or Timp1 (Mm00441818_m1). Actb- or 18S rRNA-normalized mRNA concentrations were calculated using the ΔCT for the median of technical triplicate cycle-threshold intercepts (CT's) from target and endogenous control genes.

For microarray expression profiling, biotinylated cRNA were prepared from 250ng of purified total RNA using the GeneChip 3'IVT Express Kit (Affymetrix, Santa Clara, CA) according the manufacturer's standard protocol. Following fragmentation, labeled cRNA were hybridized on Affymetrix Mouse Genome 430A 2.0 microarrays using the Affymetrix GeneChip Hybridization, Wash, and Stain Kit and standard protocol. Hybridization was performed for 16h at 45°C, 60rpm in an Affymetrix GeneChip Hybridization Oven 640 and staining and washing were performed using an Affymetrix GeneChip Fluidics Station 450 using recommended fluidics script FS450_0002. GeneChips were scanned in an Affymetrix GeneChip Scanner 7G using AGCC software and resulting CEL files were exported to GCOS v1.4.0.036 to generate CEL files compatible with Agilent GeneSpring GX 7.3.1 analysis software. CEL data were preprocessed using the GC content-based Robust Multi-Array (GCRMA) algorithm and imported into GeneSpring GX 7.3.1. GCRMA-processed, median-normalized data and raw CEL files are available at http://www.ncbi.nlm.nih.gov/geo/query/acc.cgi?acc=GSE68857. Low intensity probesets with mean raw fluorescence values ≤50 in all groups were filtered from further analysis. Between-group gene expression comparisons were performed on median per-gene normalized data using parametric t-tests without assuming equal variances or correcting for multiple comparisons. FG-3149-responsive cardiac injury genes were defined as genes with a >2-fold difference in expression in IgG-treated PKCε mice vs. IgG-treated FVB mice at $P<0.05$ that were also resolved >1.5-fold at $P<0.05$ in FG-3149-treated vs. IgG-treated PKCε mice.

SUPPLEMENTAL RESULTS

Online Figure I

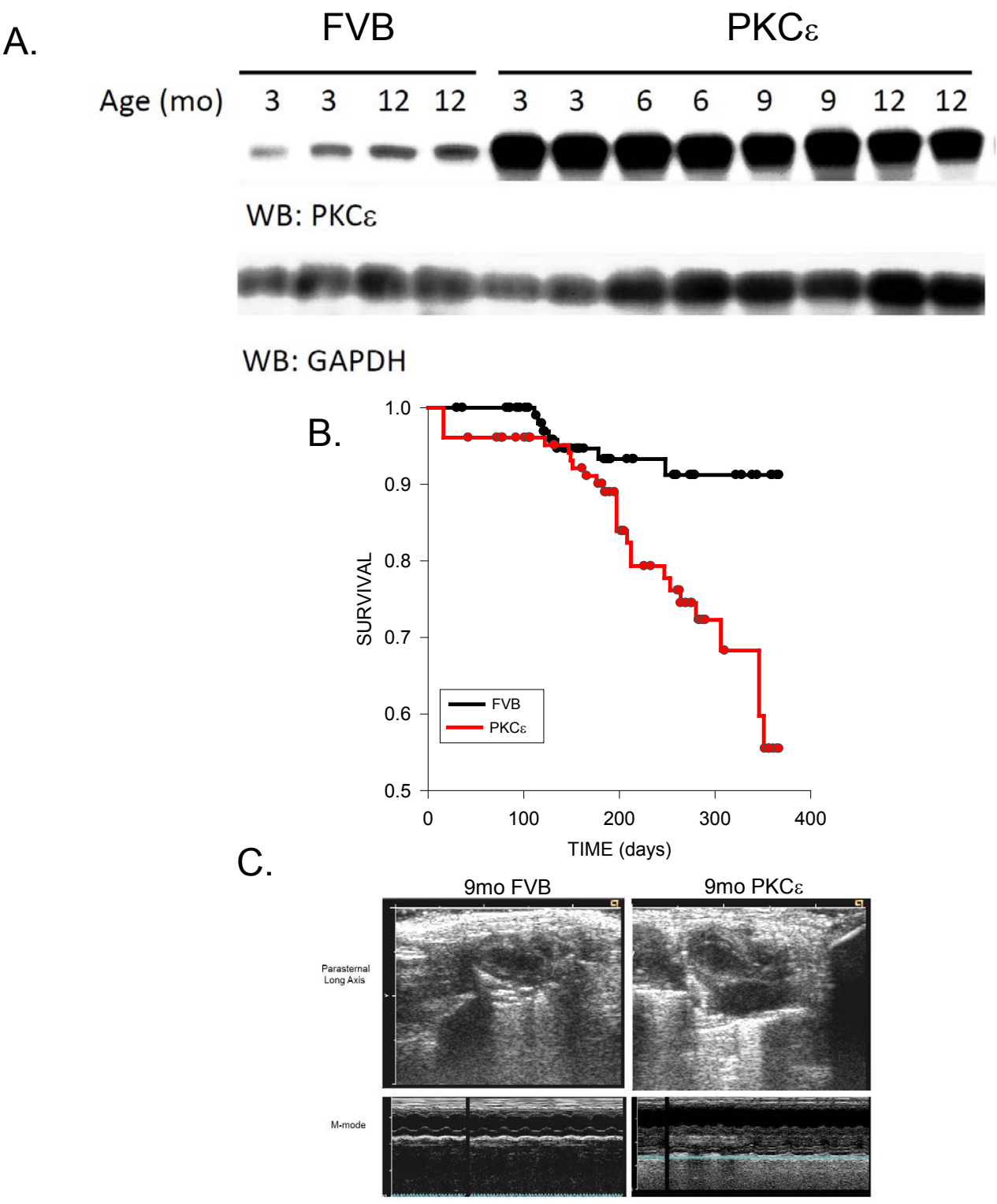

Online Figure I. *PKCε mice have a dilated cardiomyopathy with increased mortality.* (A) Western blot of LV tissue extracts (50μg of total protein per lane) from FVB and PKCε mice of varying ages (3-12mo). (B) Kaplan-Meier survival curves for FVB (n=131) and PKCε (n=128) mice. Nontransgenic FVB mice had a mean survival time of 349±7 days, whereas PKCε transgenic mice mean survival time was 310±10 days (P<0.001; Log-Rank Test). Most deaths occurred suddenly and unexpectedly. (C) Representative M-mode and 2-D echocardiograms of 9mo FVB and PKCε mice demonstrated that PKCε mice have a dilated cardiomyopathy with all 4 chambers affected.

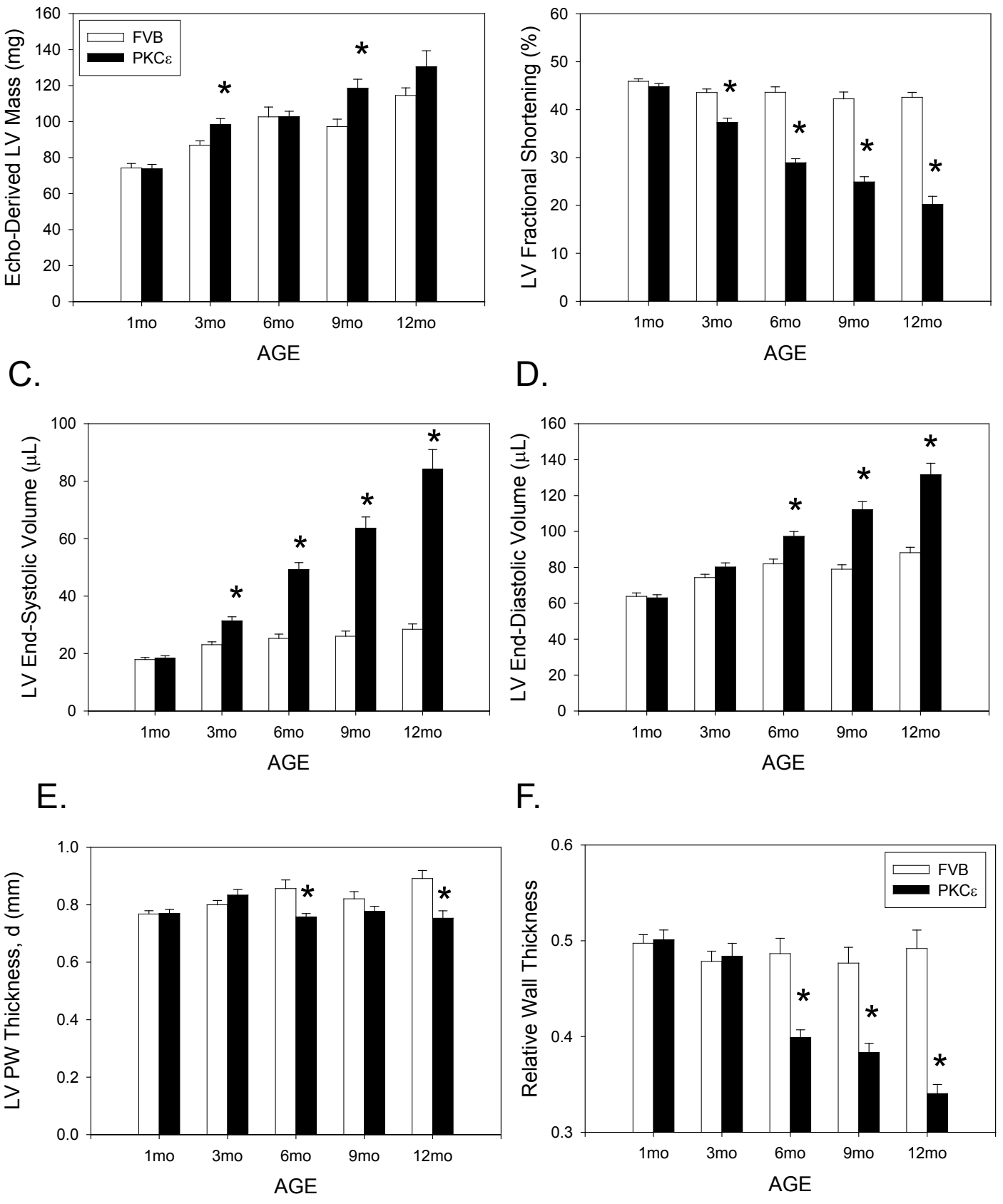
A.
B.
C.
D.
E.
F.
FVB
PKCε
Echo-Derived LV Mass (mg)
LV Fractional Shortening (%)
LV End-Systolic Volume (μL)
LV End-Diastolic Volume (μL)
LV PW Thickness, d (mm)
Relative Wall Thickness
1mo
3mo
6mo
9mo
12mo
AGE
*

G.

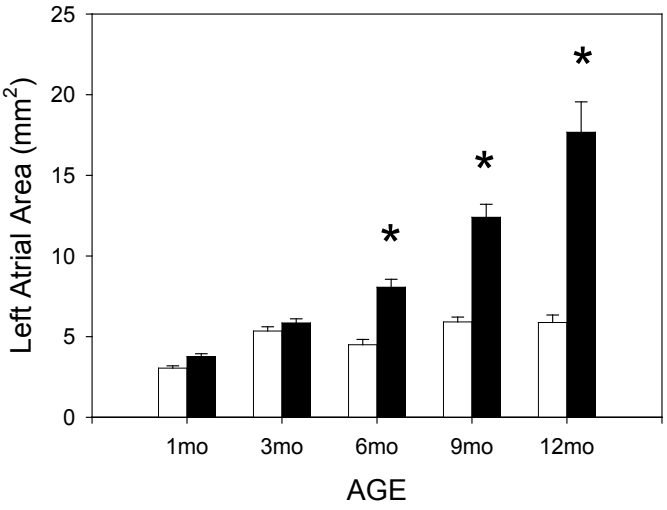

H.

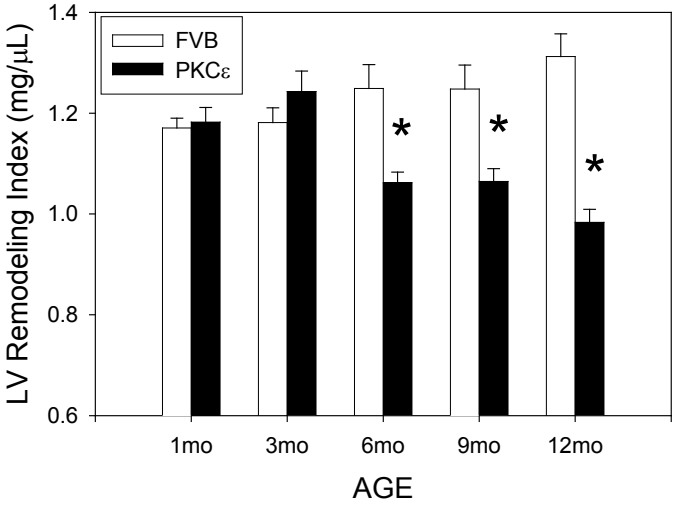

Online Figure II. *PKCε mice develop a dilated cardiomyopathy with LV systolic and diastolic dysfunction.* Serial M-mode and 2D echocardiography were used to assess the age at which LV dysfunction developed in PKCε mice. (A) Echo-derived LV mass was similar in PKCε and FVB mice at 1 month and modestly increased at 3 months of age, indicating that this level of PKCε over-expression produced only mild LV hypertrophy. (B) PKCε expression significantly reduced LV FS beginning at 3 months of age. (C) The reduced FS was initially the result of increased LV end-systolic dimension and LVESV, suggesting a primary defect in contractility. (D) Thereafter, LV end-diastolic dimension and LVEDV increased, (E) together with a small decrease in LV posterior wall (PW) thickness, (F) along with a much larger decrease in relative wall thickness as the chamber dilated. (G) By 12 months of age, surviving PKCε mice demonstrated a profoundly increased left atrial area, and (H) a substantial decrease in LVRI. *$P<0.05$ for FVB vs. PKCε by 2-way ANOVA followed by Holm-Sidak test.

Online Table I. Systolic and Diastolic Function in FVB and PKCε Mice

Parameter	3 mo		6 mo		9 mo		12 mo	
	FVB	**PKCε**	**FVB**	**PKCε**	**FVB**	**PKCε**	**FVB**	**PKCε**
n=	12	7	17	19	9	28	14	10
Heart Rate (bpm)	578±9	528±27	516±8	484±13	510±15	456±12*	525±22	411±27*
$+dP/dt_{max}$ (mmHg x sec^{-1})	11923±586	8138±1051*	11595±742	6192±534*	10517±815	5624±292*	10548±815	5306±725*
Contractility Index (sec^{-1})	169±9	132±11*	147±4	97±4*	158±7	90±3*	151±5	88±6*
$-dP/dt_{max}$ (mmHg x sec^{-1})	-9262±1028	-6894±729*	-8477±636	-5070±395*	-7380±695	-4318±301*	-7360±610	-3988±434*
Tau ($msec^{-1}$)	6.1±0.2	9.9±2.2	7.1±0.8	12.8±0.8*	7.4±0.7	15.3±1.2*	7.5±0.5	14.2±1.3*
Maximum Systolic Pressure (mmHg)	114±14	91±3	129±8	98±6*	112±10	93±4	108±5	88±7
End-diastolic Pressure (mmHg)	2±1	6±1	3±2	10±2*	4±1	11±1*	4±1	12±3*
End-diastolic volume (µl)	56±9	45±5	54±4	73±3*	48±3	74±3*	57±3	86±11*

Online Table I. *LV pressure/volume analysis confirmed the deleterious effects of PKCε expression on LV performance.* FVB and PKCε mice were subjected to LV catheterization under general anesthesia via a subdiaphragmatic approach using a 1.4F pressure-volume catheter. Systolic and diastolic function were both significantly impaired in 3 month-old PKCε mice, with functional indices exhibiting further progressive declines over the next 9 months. In contrast, systolic and diastolic indices remained relatively constant in FVB mice over the same observation period. By 12 months, most surviving PKCε mice demonstrated gross left atrial enlargement, pleural and pericardial effusions, and ascites. n, number of experimental animals in each group; bpm, beats per minute; Contractility Index, defined as dP/dt_{max} / P at dP/dt_{max}; *P<0.05, FVB vs. PKCε for each age level by 2-way ANOVA followed by the Holm-Sidak test.

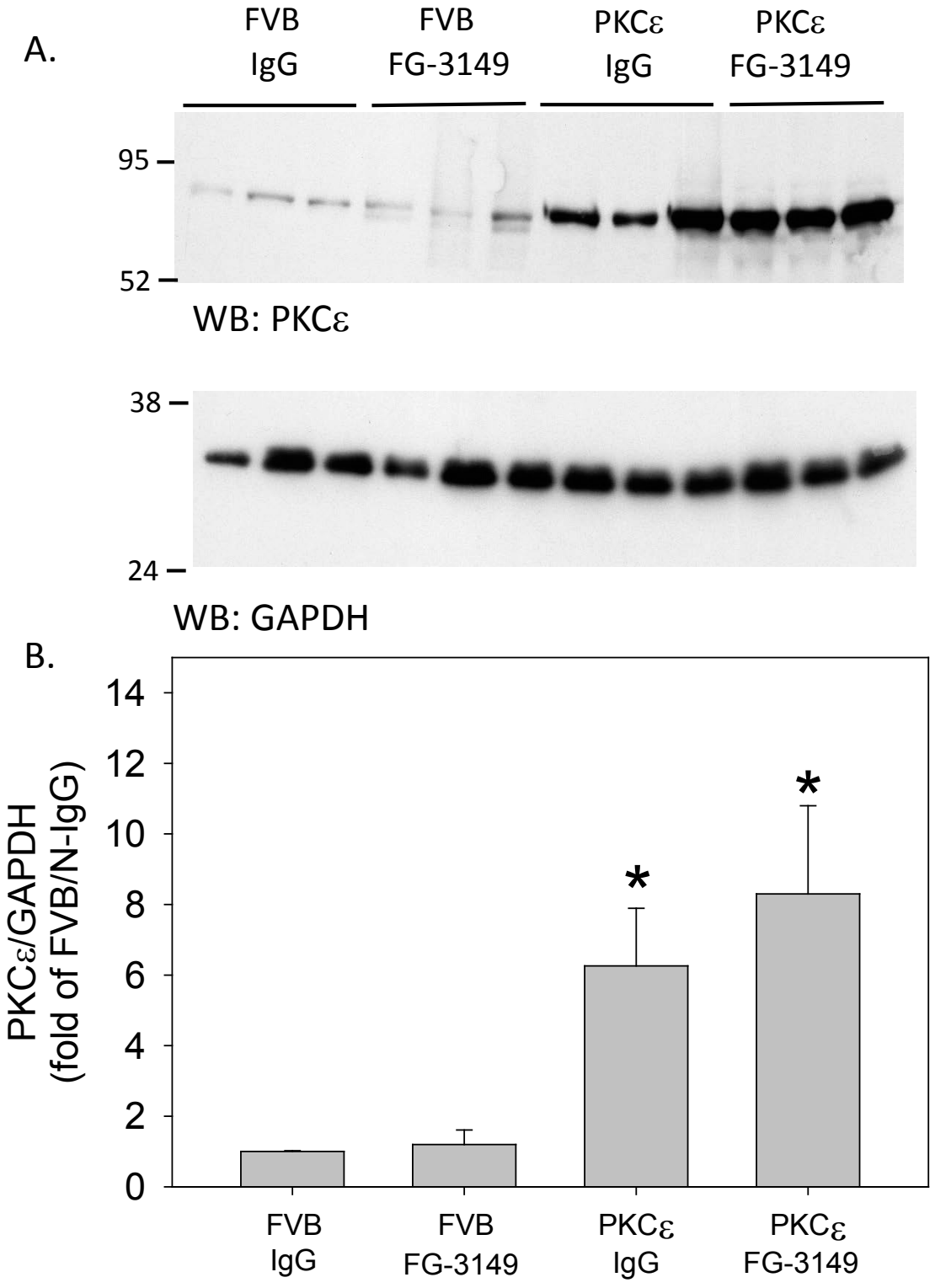

Online Figure III. *FG-3149 has no effect on PKCε expression.* 3mo FVB and PKCε mice were administered control IgG (IgG; 30mg/kg IP twice weekly for 3mo) or FG-3149, a mouse-specfic, neutralizing mAb to CTGF (30mg/kg IP twice weekly for 3mo). LV tissue extracts were then analyzed by for PKCε expression by Western blotting. (A) Representative Western blot for 3 animals in each group. (B) Quantitative analysis of PKCε expression (relative to GAPDH) in n=6 mice in each group. *P<0.05 vs. FVB+IgG by 2-way ANOVA followed by the Holm-Sidak test.

Online Figure IV

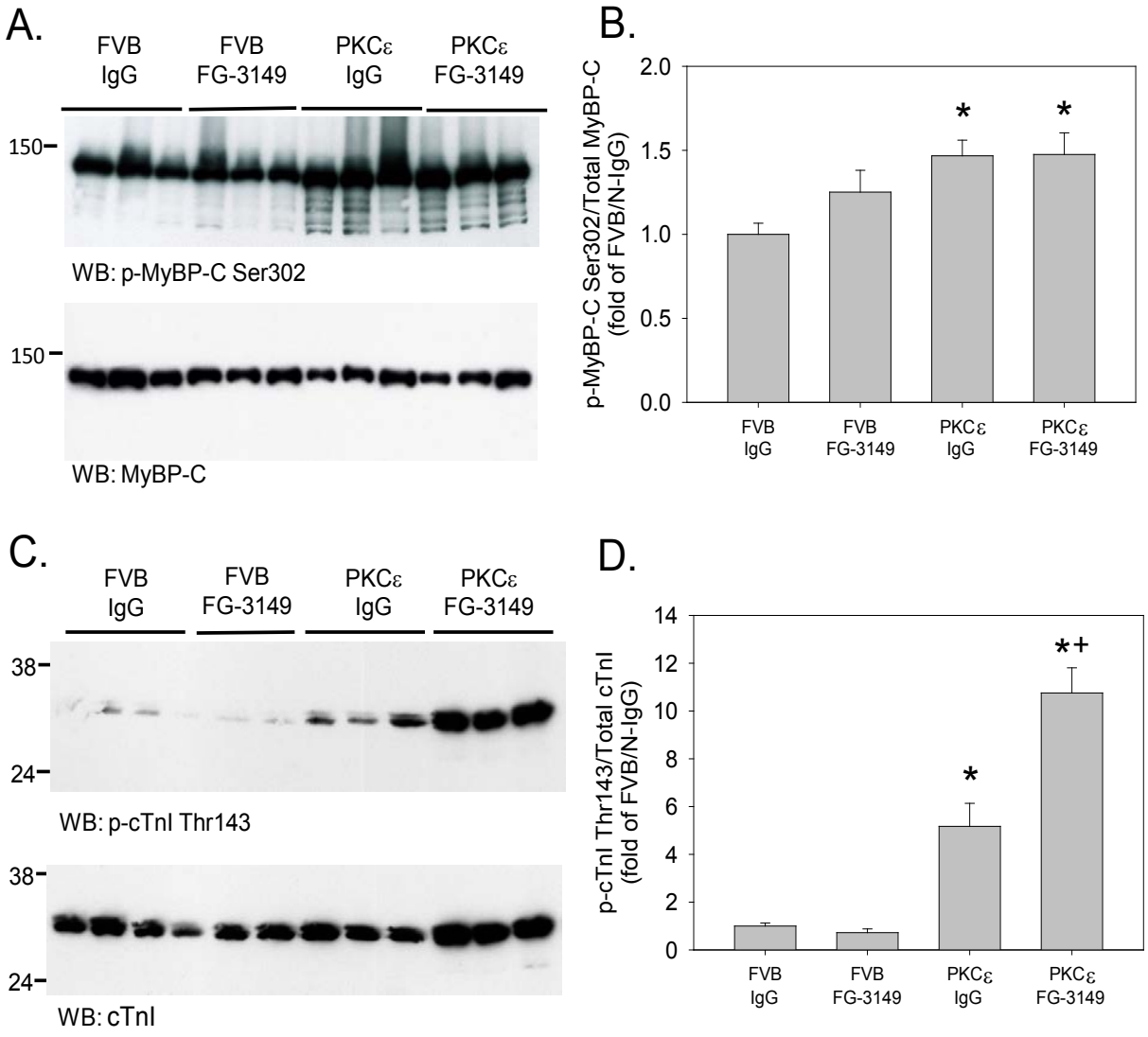

Online Figure IV. *Effects of PKCε and FG-3149 on myofilament phosphorylation.* 3 mo FVB and PKCε mice were administered control IgG (IgG; 30mg/kg IP) or FG-3149 (30mg/kg IP), a mouse-specific, neutralizing mAb to CTGF, twice weekly for a period of 3 mo. LV tissue extracts were then analyzed for MyBP-C and cTnI phosphorylation by Western blotting. (A) Representative Western blot of MyBP-C phosphorylation at Ser302 for 3 animals in each group. (B) Quantitative analysis of of MyBP-C Ser302 phosphorylation in n=9 mice in each group. (C) Representative Western blot of cTnI Thr143 phosphorylation for 3 animals in each group. (D) Quantitative analysis of cTnI Thr143 phosphorylation in n=9 mice in each group. **P*<0.05 vs. FVB-IgG; $^{+}$*P*<0.05 vs. PKCε-IgG by 2-way ANOVA followed by the Holm-Sidak test.

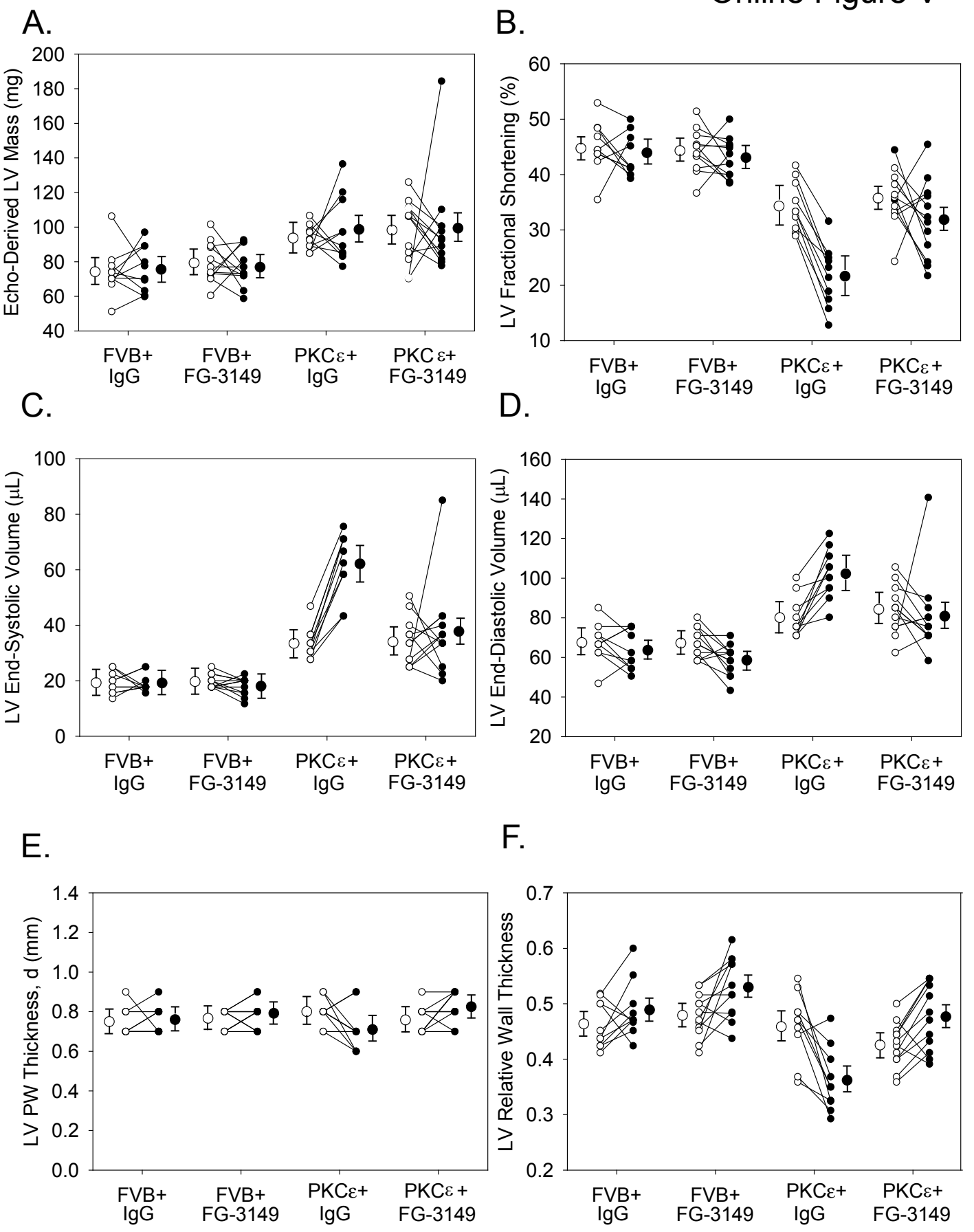
A.
Echo-Derived LV Mass (mg)
200
180
160
140
120
100
80
60
40
FVB+ IgG
FVB+ FG-3149
PKCε+ IgG
PKCε+ FG-3149
B.
LV Fractional Shortening (%)
60
50
40
30
20
10
FVB+ IgG
FVB+ FG-3149
PKCε+ IgG
PKCε+ FG-3149
C.
LV End-Systolic Volume (μL)
100
80
60
40
20
0
FVB+ IgG
FVB+ FG-3149
PKCε+ IgG
PKCε+ FG-3149
D.
LV End-Diastolic Volume (μL)
160
140
120
100
80
60
40
20
FVB+ IgG
FVB+ FG-3149
PKCε+ IgG
PKCε+ FG-3149
E.
LV PW Thickness, d (mm)
1.4
1.2
1.0
0.8
0.6
0.4
0.2
0.0
FVB+ IgG
FVB+ FG-3149
PKCε+ IgG
PKCε+ FG-3149
F.
LV Relative Wall Thickness
0.7
0.6
0.5
0.4
0.3
0.2
FVB+ IgG
FVB+ FG-3149
PKCε+ IgG
PKCε+ FG-3149

G.

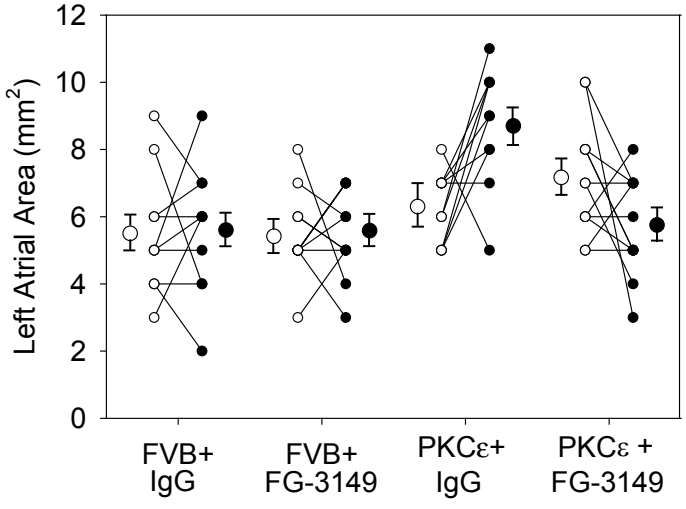

H.

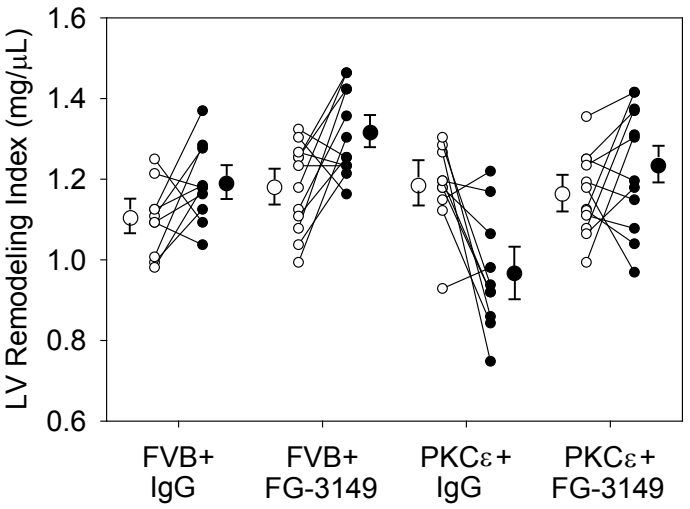

Online Figure V. *CTGF neutralizing antibody maintains LV function and slows the progression of LV remodeling in PKCε mice.* 3 month old FVB (n=22) and PKCε (n=22) mice underwent baseline M-mode and 2-D echocardiography and were then randomly assigned to receive nonimmune mouse IgG (IgG; 30mg/kg IP) or FG-3149 (30mg/kg IP), a neutralizing mAb to CTGF. Animals were treated twice weekly for a period of 3 months, and were then subjected to repeat M-mode and 2-D echocardiography. Data are responses of individual animals for each parameter before (○) and after (●) treatment. (A) LV Mass (mg); (B) LV Fractional Shortening (%); ((C) LV End-Systolic Volume (μL); (D) LV End-Diastolic Volume (μL); (E) LV Posterior Wall Thickness (mm); (F) LV Relative Wall Thickness; (G) Left Atrial Area (mm^2); and (H) LV Remodeling Index (mg/μL). Mean data±SEM for n=10-12 mice in each treatment group are depicted as well.

Online Table II. FG-3149 Responsive Cardiac Injury Genes

Array probesets (n =182) with mean raw fluorescence values >50 in at least one group that were also significantly and substantially altered in IgG-treated PKCε vs IgG-treated FVB animals and significantly altered by FG-3149 vs IgG in PKCε mice were identified as described in the Materials and Methods. Fold-change (Fc), percent of Fc reversed by FG-3149 (%), and parametric p values are provided. P values were calculated without assuming equal variances or adjusting for multiple comparisons. Fc and p values are also provided for human gene orthologs that were similarly elevated or diminished at p <0.05 (or the probeset with the greatest significant Fc if multiple probesets were altered for a given human homolog) in the 74 ischemic, idiopathic dilated, hypertrophic, post-partum and viral cardiomyopathy samples vs 14 non-failing heart samples in the Harvard Cardiogenomics dataset (NCBI GEO Series GSE1145). Genes with bold lettering had expression patterns that were confirmed by qPCR.

		Effect of PKCε		PKCε Effect Resolved by FG-3149		Altered in Human Cardiomyopathies		
Affymetrix ID	Gene ID	Fc	*p*	%	*p*	Fc	*p*	Description
Genes elevated in caPKC ε hearts and partially resolved by FG-3149								
1418476_at	Crlf1	8.3	< 0.0001	66	0.005			cytokine receptor-like factor 1
1418061_at	**Ltbp2**	6.3	< 0.0001	86	0.0008	2.7	< 0.0001	latent transforming growth factor beta binding protein 2
1451922_at	Lman1l	6.2	< 0.0001	43	0.0009			lectin, mannose-binding 1 like
1418440_at	Col8a1	4.7	< 0.0001	48	0.005	1.8	< 0.0001	collagen, type VIII, alpha 1
1449388_at	Thbs4	4.6	< 0.0001	29	0.03	2.1	< 0.0001	thrombospondin 4
1427910_at	Cst6	4.5	< 0.0001	56	0.007			cystatin E/M
1425039_at	Itgbl1	4.4	< 0.0001	52	0.01	7.7	< 0.0001	integrin, beta-like 1
1417595_at	Meox1	4.4	< 0.0001	57	0.006			mesenchyme homeobox 1
1423606_at	**Postn**	4.4	< 0.0001	66	0.02	2.8	< 0.0001	periostin, osteoblast specific factor
1418937_at	Dio2	4.2	0.001	89	0.009	1.5	0.002	deiodinase, iodothyronine, type II
1448254_at	Ptn	4.0	< 0.0001	41	0.04	3.3	< 0.0001	pleiotrophin
1460227_at	**Timp1**	3.7	0.0009	88	0.006			tissue inhibitor of metalloproteinase 1
1456062_at	Nppa	3.7	0.01	47	0.003	2.4	0.003	natriuretic peptide type A
1423110_at	**Col1a2**	3.7	< 0.0001	48	0.003	2.1	0.002	collagen, type I, alpha 2
1427256_at	Vcan	3.7	< 0.0001	61	0.006			versican
1450625_at	**Col5a2**	3.5	< 0.0001	59	0.005	1.7	0.001	collagen, type V, alpha 2
1459546_s_at	Enpp1	3.3	< 0.0001	51	0.02			ectonucleotide pyrophosphatase/phosphodiesterase 1
1416600_a_at	Rcan1	3.3	< 0.0001	56	< 0.0001			regulator of calcineurin 1
1421694_a_at	Vcan	3.3	< 0.0001	63	0.008			versican
1449380_at	Pacsin1	3.2	< 0.0001	39	0.04			protein kinase C and casein kinase substrate in neurons 1
1419466_at	Nkd2	3.2	0.0006	70	0.04			naked cuticle 2 homolog (Drosophila)
1416688_at	Snap91	3.2	< 0.0001	39	0.0003			synaptosomal-associated protein 91
1448169_at	Krt18	3.1	0.0009	68	0.03			keratin 18
1428922_at	Tril	3.1	< 0.0001	54	< 0.0001	2.4	< 0.0001	TLR4 interactor with leucine-rich repeats
1426754_x_at	Ckap4	3.1	< 0.0001	28	0.009			cytoskeleton-associated protein 4
1418796_at	Clec11a	3.0	0.0002	66	0.03			C-type lectin domain family 11, member a
1452181_at	Ckap4	3.0	< 0.0001	31	0.009			cytoskeleton-associated protein 4
1423352_at	Crispld1	2.9	0.0003	72	0.02			cysteine-rich secretory protein LCCL domain containing 1
1423407_a_at	Fbln2	2.9	< 0.0001	49	0.0002	2.3	0.002	fibulin 2
1416666_at	**Serpine2**	2.9	< 0.0001	54	< 0.0001	1.4	< 0.0001	serine (or cysteine) peptidase inhibitor, clade E, member 2
1455494_at	**Col1a1**	2.9	< 0.0001	58	< 0.0001	2.3	< 0.0001	collagen, type I, alpha 1
1460208_at	**Fbn1**	2.9	< 0.0001	69	< 0.0001			fibrillin 1
1448475_at	Olfml3	2.8	< 0.0001	41	0.01	1.8	0.002	olfactomedin-like 3
1427257_at	Vcan	2.8	< 0.0001	59	0.02			versican
1427884_at	**Col3a1**	2.8	< 0.0001	69	0.0002	2.0	0.0005	collagen, type III, alpha 1
1448259_at	Fstl1	2.8	< 0.0001	57	0.006	1.5	0.03	follistatin-like 1
1424704_at	Runx2	2.7	< 0.0001	31	0.03	1.7	< 0.0001	runt related transcription factor 2
1422324_a_at	Pthlh	2.7	0.0006	72	0.02			parathyroid hormone-like peptide
1422437_at	**Col5a2**	2.7	< 0.0001	52	0.01	1.7	0.0009	collagen, type V, alpha 2
1448323_a_at	Bgn	2.7	< 0.0001	50	0.009	1.6	0.0003	biglycan
1428074_at	Tmem158	2.6	< 0.0001	75	0.004			transmembrane protein 158
1452436_at	Loxl2	2.6	< 0.0001	45	0.02	1.4	0.01	lysyl oxidase-like 2
1426755_at	Ckap4	2.6	< 0.0001	57	< 0.0001			cytoskeleton-associated protein 4
1416405_at	Bgn	2.6	< 0.0001	45	0.01	1.6	0.0003	biglycan
1456307_s_at	Adcy7	2.6	< 0.0001	49	0.008	1.3	0.02	adenylate cyclase 7
1424950_at	Sox9	2.6	< 0.0001	42	0.03			SRY-box containing gene 9
1417343_at	Fxyd6	2.6	< 0.0001	48	< 0.0001	1.4	0.008	FXYD domain-containing ion transport regulator 6
1418538_at	Kdelr3	2.5	< 0.0001	43	0.02	1.4	0.01	KDEL (Lys-Asp-Glu-Leu) endoplasmic reticulum protein retention receptor 3
1427298_at	Dnm3os	2.5	< 0.0001	71	0.006			dynamin 3, opposite strand
1416529_at	Emp1	2.5	< 0.0001	48	0.004			epithelial membrane protein 1
1434089_at	Synpo	2.5	< 0.0001	60	0.01			synaptopodin
1448590_at	Col6a1	2.5	< 0.0001	39	0.009	1.3	0.001	collagen, type VI, alpha 1
1438789_s_at	Dpysl3	2.5	< 0.0001	65	0.007	2.2	0.0003	dihydropyrimidinase-like 3
1419123_a_at	Pdgfc	2.5	0.0009	90	< 0.0001	1.2	0.04	platelet-derived growth factor, C polypeptide
1416221_at	Fstl1	2.5	< 0.0001	62	0.003	1.5	0.03	follistatin-like 1
1421045_at	Mrc2	2.5	< 0.0001	53	0.0005	1.5	0.0007	mannose receptor, C type 2
1455019_x_at	Ckap4	2.5	< 0.0001	47	< 0.0001			cytoskeleton-associated protein 4
1416069_at	Pfkp	2.4	< 0.0001	43	0.005			phosphofructokinase, platelet
1417507_at	Cyb561	2.4	< 0.0001	60	< 0.0001			cytochrome b-561
1425896_a_at	**Fbn1**	2.4	< 0.0001	72	< 0.0001	1.5	< 0.0001	fibrillin 1
1452250_a_at	Col6a2	2.4	< 0.0001	42	0.006	1.2	0.04	collagen, type VI, alpha 2
1451538_at	Sox9	2.4	< 0.0001	41	0.003			SRY-box containing gene 9
1415877_at	Dpysl3	2.4	< 0.0001	68	0.0006	2.2	0.0003	dihydropyrimidinase-like 3
1449351_s_at	Pdgfc	2.4	0.0008	82	0.0005	1.2	0.04	platelet-derived growth factor, C polypeptide
1420371_at	Sntb2	2.4	< 0.0001	70	< 0.0001	1.7	< 0.0001	syntrophin, basic 2
1453839_a_at	Pi16	2.4	< 0.0001	65	0.005	1.4	0.004	peptidase inhibitor 16
1448433_a_at	Pcolce	2.4	< 0.0001	53	0.001	1.6	0.006	procollagen C-endopeptidase enhancer protein
1438651_a_at	Aplnr	2.4	< 0.0001	52	0.001			apelin receptor
1417534_at	Itgb5	2.4	< 0.0001	27	0.03	1.6	0.01	integrin beta 5
1451978_at	Loxl1	2.4	< 0.0001	48	0.006	1.4	0.02	lysyl oxidase-like 1
1450857_a_at	**Col1a2**	2.4	< 0.0001	37	0.02	2.1	0.002	collagen, type I, alpha 2

1460285_at	Itga9	2.4	< 0.0001	36	0.02			integrin alpha 9
1454613_at	Dpysl3	2.4	0.0001	58	0.02	2.2	0.0003	dihydropyrimidinase-like 3
1448228_at	**Lox**	2.4	0.006	89	0.02	1.8	0.0009	lysyl oxidase
1427034_at	Ace	2.3	< 0.0001	43	0.0002			angiotensin I converting enzyme (peptidyl-dipeptidase A) 1
1451596_a_at	Sphk1	2.3	< 0.0001	68	0.005			sphingosine kinase 1
1418269_at	Loxl3	2.3	0.0001	76	0.005			lysyl oxidase-like 3
1437165_a_at	Pcolce	2.3	< 0.0001	54	0.0009	1.6	0.006	procollagen C-endopeptidase enhancer protein
1426784_at	Trim47	2.3	< 0.0001	48	0.02			tripartite motif-containing 47
1452382_at	Dnm3os	2.3	< 0.0001	64	0.003			dynamin 3, opposite strand
1437889_x_at	Bgn	2.3	< 0.0001	45	0.01	1.6	0.0003	biglycan
1416379_at	Panx1	2.3	0.0002	74	0.009			pannexin 1
1434479_at	Col5a1	2.3	< 0.0001	37	0.002	1.6	0.0002	collagen, type V, alpha 1
1416740_at	Col5a1	2.3	< 0.0001	45	0.0006	1.6	0.0002	collagen, type V, alpha 1
1417455_at	**Tgfb3**	2.3	0.0004	65	0.02	1.2	0.01	transforming growth factor, beta 3
1421037_at	Npas2	2.3	0.002	114	< 0.0001			neuronal PAS domain protein 2
1416414_at	Emilin1	2.3	< 0.0001	43	0.02			elastin microfibril interfacer 1
1424414_at	Ogfrl1	2.3	< 0.0001	38	0.0001	1.6	< 0.0001	opioid growth factor receptor-like 1
1448655_at	Lrp1	2.2	< 0.0001	40	0.01			low density lipoprotein receptor-related protein 1
1456195_x_at	Itgb5	2.2	< 0.0001	35	0.003	1.6	0.01	integrin beta 5
1426399_at	Vwa1	2.2	< 0.0001	32	0.0004			von Willebrand factor A domain containing 1
1422705_at	Pmepa1	2.2	< 0.0001	53	0.03	1.4	0.05	prostate transmembrane protein, androgen induced 1
1456133_x_at	Itgb5	2.2	< 0.0001	42	0.0008	1.6	0.01	integrin beta 5
1417533_a_at	Itgb5	2.2	< 0.0001	29	0.01	1.6	0.01	integrin beta 5
1452357_at	Gp1bb / Sept5	2.2	< 0.0001	61	0.003			glycoprotein Ib, beta polypeptide / septin 5
1423585_at	Igfbp7	2.2	< 0.0001	47	0.008	1.2	0.002	insulin-like growth factor binding protein 7
1449022_at	Nes	2.2	< 0.0001	45	0.02			nestin
1416165_at	Rab31	2.2	< 0.0001	45	< 0.0001			RAB31, member RAS oncogene family
1448428_at	Nbl1	2.2	0.001	71	0.04	1.5	< 0.0001	neuroblastoma, suppression of tumorigenicity 1
1423429_at	Rhox5	2.2	< 0.0001	43	0.02			reproductive homeobox 5
1419665_a_at	Nupr1	2.2	0.003	73	0.04			nuclear protein 1
1424131_at	Col6a3	2.2	< 0.0001	30	0.01			collagen, type VI, alpha 3
1416805_at	Fam198b	2.1	< 0.0001	41	0.04			family with sequence similarity 198, member B
1435110_at	Unc5b	2.1	< 0.0001	51	0.02	1.4	< 0.0001	unc-5 homolog B (C. elegans)
1423341_at	Cspg4	2.1	< 0.0001	53	0.0008			chondroitin sulfate proteoglycan 4
1427418_a_at	Hif1a	2.1	< 0.0001	19	0.02			hypoxia inducible factor 1, alpha subunit
1448931_at	F2rl1	2.1	0.0003	60	0.03			coagulation factor II (thrombin) receptor-like 1
1424413_at	Ogfrl1	2.1	< 0.0001	26	0.03	1.6	< 0.0001	opioid growth factor receptor-like 1
1455271_at	Gm13889	2.1	< 0.0001	56	0.003			predicted gene 13889
1448698_at	Ccnd1	2.1	< 0.0001	33	0.01	1.5	0.001	cyclin D1
1448395_at	Sfrp1	2.0	< 0.0001	52	0.02	2.1	0.01	secreted frizzled-related protein 1
1439191_at	---	2.0	0.007	104	0.0008			---
1426926_at	Plcg2	2.0	< 0.0001	25	0.03			phospholipase C, gamma 2
1451289_at	Dclk1	2.0	0.002	69	0.03			doublecortin-like kinase 1
1423790_at	Dap	2.0	0.0003	56	0.01			death-associated protein
1416759_at	Mical1	2.0	< 0.0001	44	0.009			microtubule associated monoxygenase, calponin and LIM domain containing 1
1452368_at	Bcr	2.0	0.0004	62	0.04			breakpoint cluster region
1450355_a_at	Capg	2.0	< 0.0001	50	0.03			capping protein (actin filament), gelsolin-like
1449002_at	Phlda3	2.0	< 0.0001	45	0.02			pleckstrin homology-like domain, family A, member 3
1449281_at	Nrtn	2.0	0.003	59	0.003			neurturin
1418733_at	Twist1	2.0	< 0.0001	49	0.009			twist homolog 1 (Drosophila)
1452035_at	Col4a1	2.0	< 0.0001	66	< 0.0001			collagen, type IV, alpha 1
Genes diminished in caPKC ε hearts and partially resolved by FG-3149								
1449081_at	Ces1d	0.15	< 0.0001	17	0.001			carboxylesterase 1D
1435370_a_at	Ces1d	0.18	< 0.0001	15	0.02			carboxylesterase 1D
1427213_at	Pfkfb1	0.22	< 0.0001	20	0.03			6-phosphofructo-2-kinase/fructose-2,6-biphosphatase 1
1435371_x_at	Ces1d	0.26	< 0.0001	25	0.007			carboxylesterase 1D
1421928_at	Epha4	0.27	< 0.0001	22	< 0.0001			Eph receptor A4
1424737_at	Thrsp	0.27	< 0.0001	7	0.008			thyroid hormone responsive SPOT14 homolog (Rattus)
1423085_at	Efnb3	0.28	0.0001	27	0.03			ephrin B3
1453678_at	Mbd1	0.30	< 0.0001	19	0.03	0.68	0.01	methyl-CpG binding domain protein 1
1421929_at	Epha4	0.31	< 0.0001	10	0.03			Eph receptor A4
1422973_a_at	Thrsp	0.32	< 0.0001	10	0.006			thyroid hormone responsive SPOT14 homolog (Rattus)
1455061_a_at	Acaa2	0.32	< 0.0001	35	0.007			acetyl-Coenzyme A acyltransferase 2
1421063_s_at	Snrpn / Snurf	0.33	< 0.0001	41	< 0.0001	0.74	0.002	small nuclear ribonucleoprotein N / SNRPN upstream reading frame
1449065_at	Acot1	0.34	< 0.0001	43	0.007			acyl-CoA thioesterase 1
1436833_x_at	Ttll1	0.34	< 0.0001	25	0.02			tubulin tyrosine ligase-like 1
1454638_a_at	Pah	0.34	0.0002	29	0.01			phenylalanine hydroxylase
1417729_at	Myh6	0.37	< 0.0001	31	0.002	0.34	< 0.0001	myosin, heavy polypeptide 6, cardiac muscle, alpha
1451270_at	Dusp18	0.37	< 0.0001	32	< 0.0001			dual specificity phosphatase 18
1460732_a_at	Ppl	0.38	0.0006	31	0.03	0.74	0.01	periplakin
1417765_a_at	Amy1	0.38	< 0.0001	39	< 0.0001			amylase 1, salivary
1426263_at	Cadm4	0.38	< 0.0001	29	0.003			cell adhesion molecule 4
1452823_at	Gstk1	0.39	< 0.0001	26	0.003			glutathione S-transferase kappa 1
1424226_at	9030617O03Rik	0.40	< 0.0001	20	0.006			RIKEN cDNA 9030617O03 gene
1421488_at	Rabgap1l	0.40	< 0.0001	24	0.02			RAB GTPase activating protein 1-like
1423183_at	Lgi1	0.41	0.005	71	0.004			leucine-rich repeat LGI family, member 1
1421468_at	Kcnj3	0.41	0.0006	24	0.002			potassium inwardly-rectifying channel, subfamily J, member 3
1418093_a_at	Egf	0.42	< 0.0001	32	0.003			epidermal growth factor
1449088_at	Fbp2	0.42	0.0002	48	0.02			fructose bisphosphatase 2
1451776_s_at	Hopx	0.42	< 0.0001	49	0.002	0.41	0.002	HOP homeobox
1427202_at	Mettl20	0.42	< 0.0001	36	< 0.0001			methyltransferase like 20
1425164_a_at	Phkg1	0.43	0.0005	29	0.01			phosphorylase kinase gamma 1
1423892_at	Apbb1	0.43	< 0.0001	27	0.01	0.82	0.01	amyloid beta (A4) precursor protein-binding, family B, member 1
1426010_a_at	Epb4.1l3	0.43	< 0.0001	38	0.0002			erythrocyte protein band 4.1-like 3
1455531_at	Mfsd4	0.43	< 0.0001	27	0.004			major facilitator superfamily domain containing 4
1423893_x_at	Apbb1	0.44	< 0.0001	27	0.01	0.82	0.01	amyloid beta (A4) precursor protein-binding, family B, member 1
1425619_s_at	Dsg2	0.44	< 0.0001	24	0.002			desmoglein 2
1449501_a_at	Gzmm	0.45	< 0.0001	11	0.03			granzyme M (lymphocyte met-ase 1)
1422996_at	Acot2	0.45	< 0.0001	48	0.005			acyl-CoA thioesterase 2

1453355_at	Wnk2	0.45	< 0.0001	22	0.01			WNK lysine deficient protein kinase 2
1427964_at	Cmtm8	0.45	< 0.0001	20	0.01			CKLF-like MARVEL transmembrane domain containing 8
1424393_s_at	Adhfe1	0.46	< 0.0001	49	0.002			alcohol dehydrogenase, iron containing, 1
1448609_at	Tst	0.46	< 0.0001	26	0.002			thiosulfate sulfurtransferase, mitochondrial
1422997_s_at	Acot1 / Acot2	0.46	< 0.0001	43	0.005			acyl-CoA thioesterase 1 / acyl-CoA thioesterase 2
1428662_a_at	Hopx	0.47	< 0.0001	45	0.004	0.41	0.002	HOP homeobox
1435716_x_at	Snrpn / Snurf	0.47	< 0.0001	21	0.007	0.74	0.002	small nuclear ribonucleoprotein N / SNRPN upstream reading frame
1424392_at	Adhfe1	0.47	< 0.0001	48	0.001			alcohol dehydrogenase, iron containing, 1
1439476_at	Dsg2	0.48	< 0.0001	22	0.04			desmoglein 2
1419209_at	Cxcl1	0.48	0.005	69	0.004	0.56	0.03	chemokine (C-X-C motif) ligand 1
1422315_x_at	Phkg1	0.48	0.001	20	0.04			phosphorylase kinase gamma 1
1449984_at	Cxcl2	0.48	0.001	39	0.02			chemokine (C-X-C motif) ligand 2
1426427_at	Ttll1	0.48	< 0.0001	19	0.009			tubulin tyrosine ligase-like 1
1428021_at	Mccc2	0.48	< 0.0001	41	0.006	0.69	0.04	methylcrotonoyl-Coenzyme A carboxylase 2 (beta)
1416154_at	Srp54a / Srp54b	0.49	< 0.0001	34	0.01			signal recognition particle 54A / signal recognition particle 54B
1460316_at	Acsl1	0.49	< 0.0001	27	0.04			acyl-CoA synthetase long-chain family member 1
1448136_at	Enpp2	0.49	0.001	22	0.03			ectonucleotide pyrophosphatase/phosphodiesterase 2
1436791_at	Wnt5a	0.49	< 0.0001	27	0.01			wingless-related MMTV integration site 5A
1448181_at	Klf15	0.49	< 0.0001	47	0.0003			Kruppel-like factor 15
1417823_at	Gcat	0.50	< 0.0001	26	0.02	0.66	0.002	glycine C-acetyltransferase (2-amino-3-ketobutyrate-coenzyme A ligase)
1428145_at	Acaa2	0.50	0.0001	37	0.02			acetyl-Coenzyme A acyltransferase 2
1422678_at	Dgat2	0.50	< 0.0001	39	0.008			diacylglycerol O-acyltransferase 2
1417702_a_at	Hnmt	0.50	< 0.0001	27	0.04			histamine N-methyltransferase

Online Figure VI

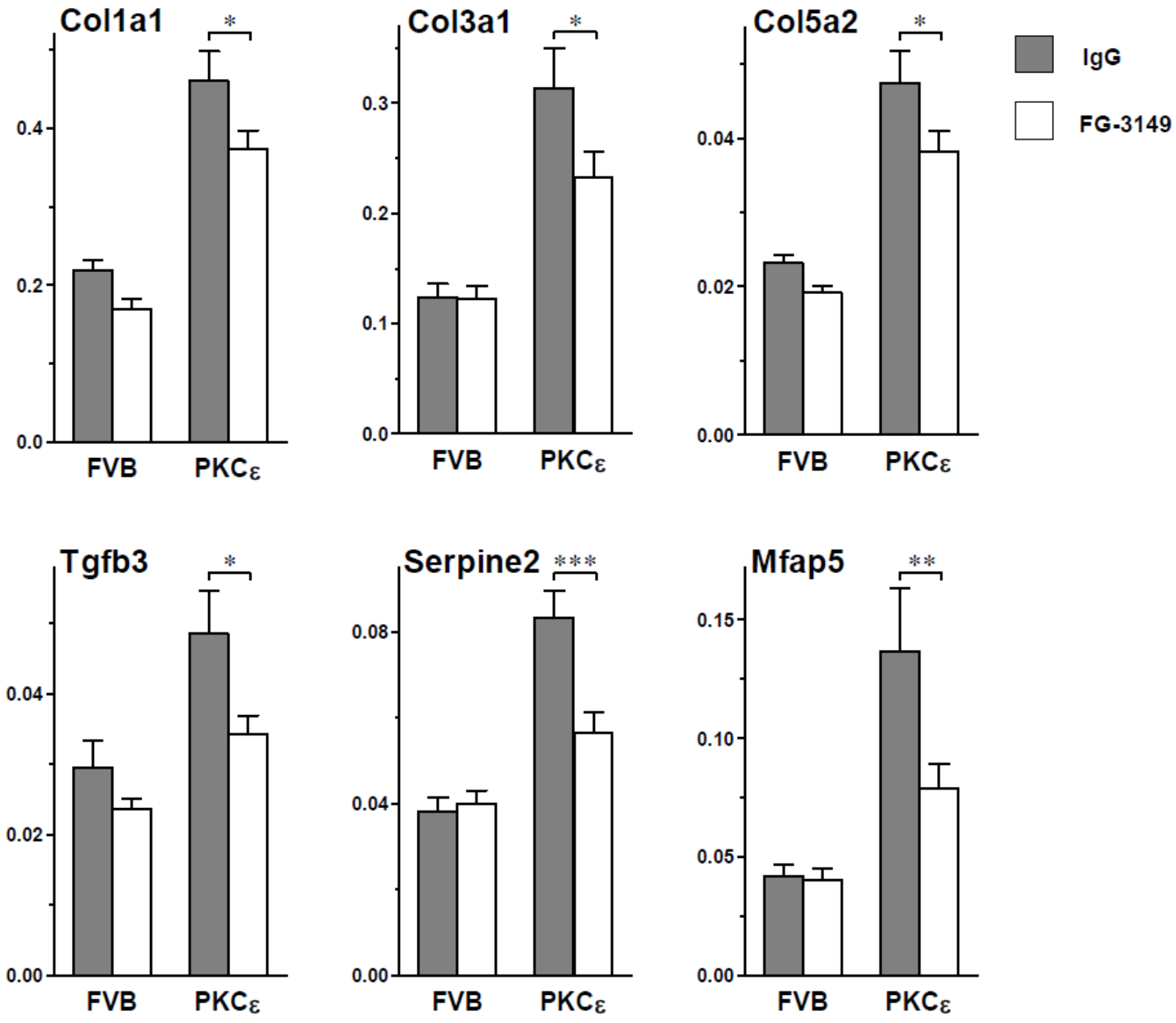

Online Figure VI. Validation of select ECM and ECM remodeling genes by qPCR. Grey and white bars indicate IgG and FG-3149 treatments, respectively. Actb-normalized expression (mean ± SEM) was altered by genotype (P<0.001) and treatment (P<0.05) for all genes (2-way ANOVA). Bonferroni post-test P<0.05 (*), 0.01 (**), 0.001(***).

Online Figure VII

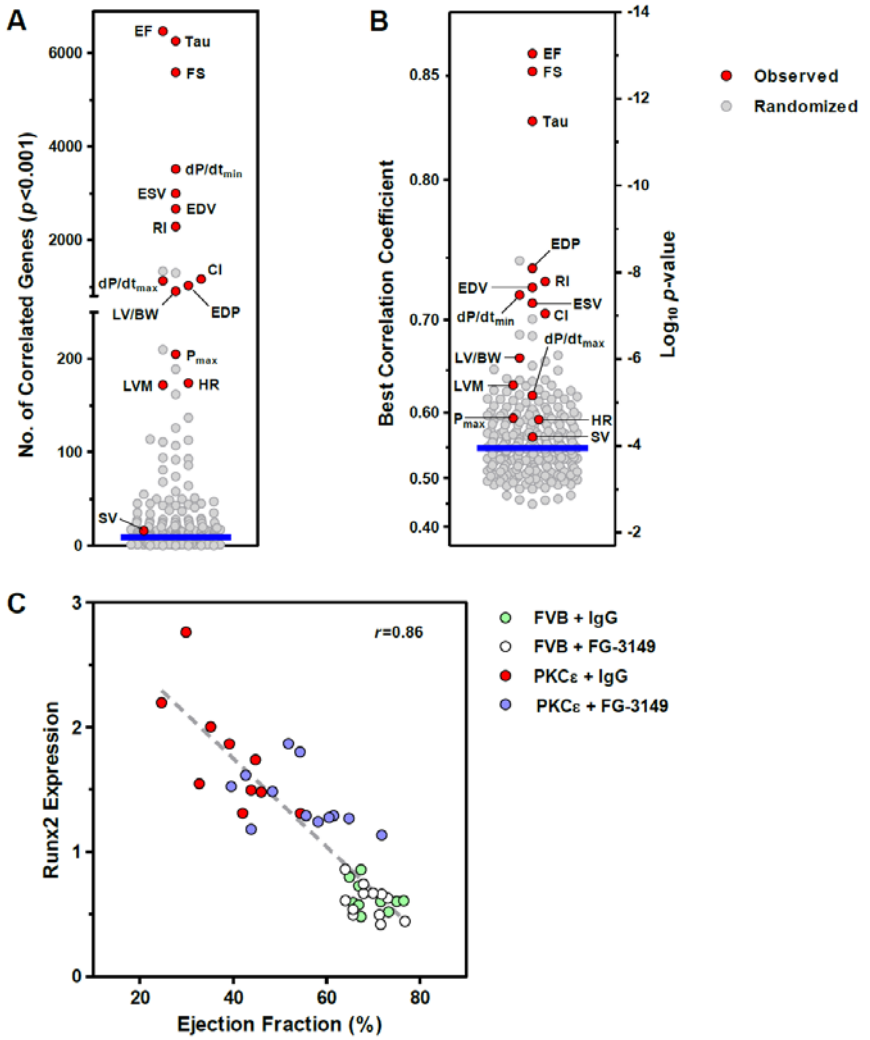

Online Figure VII. Stronger than expected associations between specific genes and FG-responsive cardiac function parameters. **A.** The number of genes correlated with cardiac parameters at *P*<0.001 (red circles) compared to the number of genes correlated with 250 randomized scenarios (grey circles). The median number of genes correlated after permutation analysis (*n*=9, blue bar) was far lower than that observed for key functional parameters (e.g., 6467 for EF). **B.** The best Pearson correlation coefficients (*r*, absolute value) and accompanying *P*-values for measured cardiac parameters (red circles) and 250 random simulations (grey circles). The median top correlation for the random scenarios (*r*=0.55) was far lower than those observed for the cardiac parameters most highly affected by PKCε and FG-3149 treatment. **C.** Median normalized expression of the gene (Runx2, runt-related transcription factor 2) most highly correlated with EF. EF, left ventricular (LV) ejection fraction; FS, LV fractional shortening; EDP, end-diastolic pressure; EDV, end-diastolic volume; ESV, end-systolic volume; CI, contractility index; RI, remodeling index; LVM, LV mass; LV/BW, LV-to-body weight ratio; P_{max}, maximum systolic pressure; dP/dt_{max}, maximum rate of LV pressure increase during the initiation of systole; dP/dt_{min}, maximum rate of LV pressure decline during the initiation of diastole; HR, heart rate; SV, stroke volume.

Online Table III. Proportional Representation of Human Cardiomyopathy Genes among FG-3149 Responsive Cardiac Injury Genes

Human Cardiomyopathy Dataset	(n, t, N, T)	Fold Enrichment	*p*	Concordant Genes
FG-3149-responsive genes elevated in both PKCε hearts and human cardiomyopathies				
Harvard Cardiogenomics (GSE1145)	(20, 237, 214, 26305)	8	7E-36	*Col1a1, Col1a2, Dpysl3, Fbln2, Itgbl1 (4), Ltbp2 (2), Nppa, Postn (3), Ptn (3), Sfrp1, Thbs4, Tril*
Hannenhalli et al. 2006 (GSE5406)	(7, 179, 22, 15685)	28	8E-32	*Col1a1, Col1a2 (2), Col3a1 (2), Nppa, Ptn*
Barth et al. 2006 (GSE3585)	(7, 107, 31, 8391)	18	2E-21	*Col1a1, Col1a2, Itgbl1, Ltbp2, Nppa, Postn, Serpine2*
Kittleson et al. 2005 (GSE1869)	(2, 179, 64, 15685)	3	ns	*Col3a1, Postn*
FG-3149-responsive genes diminished in both PKCε hearts and human cardiomyopathies				
Harvard Cardiogenomics (GSE1145)	(2, 118, 254, 26305)	2	ns	*Hopx, Myh6*
Hannenhalli et al. 2006 (GSE5406)	(2, 61, 33, 15685)	16	4E-07	*Hopx, Myh6*
Barth et al. 2006 (GSE3585)	(1, 34, 10, 8391)	25	5E-06	*Myh6*
Kittleson et al. 2005 (GSE1869)	(1, 61, 1, 15685)	257	1E-29	*Myh6*

Enrichment = (n/t)/(N/T), where n = the number of FG-3149-responsive cardiac injury gene ortholog probesets similarly altered in the indicated human dataset (Fc>2, p <0.05 vs non-failing (NF) hearts), t = total FG-3149-responsive injury gene ortholog probesets for the indicated dataset, N = number of homologous probesets altered in the indicated human dataset (Fc>2, P<0.05), and T = total probesets in the indicated dataset homologous to those on the mouse MOE430A_2.0 platform. Observed proportions of FG-3149-responsive cardiac injury genes similarly altered in the human cardiomyopathy datasets were compared to the proportions expected by chance using the $\chi 2$ statistic. Concordant genes are those FG-3149-responsive genes that were similarly altered in both PKCε hearts and human cardiomyopathy samples (Fc>2, P <0.05 each), where the number of probesets that met cut-offs in the human datasets are indicated in parentheses if greater than one. The human datasets contained data from 26 DCM, 32 ICM, 7 viral, 5 hypertrophic, 4 post-partum and 14 NF hearts (GSE1145), 108 DCM, 86 ICM and 16 NF hearts (GSE5406), 7 DCM and 5 NF hearts (GSE3585), and 21 DCM, 10 ICM and 6 NF hearts (GSE1869).